

Controllability Analysis on Functional Brain Networks

Shi Gu (gus@uestc.edu.cn)

No. 2006, Xiyuan Ave., West High-tech Zone
Chengdu, Sichuan, China

Shikuang Deng

No. 2006, Xiyuan Ave., West High-tech Zone
Chengdu, Sichuan, China

Abstract

Controllability analysis on brain networks is an emerging subfield of network neuroscience. It utilizes both the classical and modern control theories to understand the roles of control regions and their energetic properties in certain neural circuits. The previous framework is based on the structural networks built from diffusion imaging thus lacks the adaptability to the functional networks. Here, we apply the system identification algorithm to the BOLD time series to infer the effective connectivity matrix and noise structure, followed by transferring the recognized stochastic dynamics into the linear system and quantifying the controllability via the minimal control sets, the global controllability, the average controllability and the synchronizability. This work provides a complementary part of the structural controllability analysis and enables the investigation of controllability on functional brain networks.

Keywords: network; controllability; brain dynamics

Introduction

Being able to consciously control the brain states has long been human being's dream. Yet, to achieve this ultimate goal, given the constrained knowledges and instruments we can access today, it would be a more realistic target to investigate how the brain performs its own control system from both the structural and functional perspectives. Control theory allows us to probe into the type of question how the system can be driven into certain states with some input energy. This group of methods have already been applied in analyzing the general biological networks (Liu, Slotine, & Barabási, 2011), the *C.elegans* neural system (Yan et al., 2017) and human's modeled dynamics inferred diffusion spectrum imaging (Gu et al., 2015). Specially on the human brain's structural networks, there are also works that extend the dynamics with nonlinear activation functions (Muldoon et al., 2016), examine the roles of controllability through the neural development (Tang et al., 2017) and inspect its impact on the dynamical trajectories of transitioning among states (Betzler, Gu, Medaglia, Pasqualetti, & Bassett, 2016; Gu et al., 2017). On the other hand, to the best as we know, although there are already attempts on building the whole brain computational models (Deco, Tononi, Boly, & Kringelbach, 2015), the analysis from the control perspective still lacks.

In this work, we studied the problem of functional controllability with the extensively processed fMRI Data from the HCP Young Adults 1200 released subjects (Van Essen et al., 2013). We first identified the stochastic linear equation by fitting the 0- and 1-shift correlation matrices. Next, based on the fitted dynamics, we built the regular linear control system by setting up the transition matrix as the effective connectivity and formatting the control matrix as the covariance matrix of noise structure. Finally we examined the distribution of minimal control sets and three types of controllability measurements across the 1003 subjects.

Methods

We denote the state (could be BOLD signals) at time t for a brain as \mathbf{x}_t , which is an $N \times 1$ vector with N as the number of regions. Usually, the evolutionary dynamics of the states is formulated as describing the state's time derivative dx/dt with the state variable x and other parameterized related terms, e.g. the noise. In this work, we attempt to firstly fit the dynamics of \mathbf{x}_t , followed by investigating it from the control perspectives where we examine both the spatial distribution of minimal control sets and control measurements.

Construction of the Control Dynamics

Here, we start from the linear stochastic model, where the changing rate of the state is determined by the current state and the random perturbation following Gilson's setting (Gilson, Moreno-Bote, Ponce-Alvarez, Ritter, & Deco, 2016). Mathematically, the dynamic model is given by

$$d\mathbf{x} = \left(-\frac{1}{\tau_x}\mathbf{x} + \mathbf{C}\mathbf{x}\right)dt + d\mathbf{W}_t, \quad (1)$$

where τ_x is the time constant, \mathbf{C} is the effective connectivity matrix and $d\mathbf{W}$ is a wiener process with covariance Σ . Let $\mathbf{J} = -\frac{1}{\tau_x}\mathbf{I} + \mathbf{C}$ be the Jacobian. The loss function of fitting the dynamics is given by the weighted sum of the distance between each pair of estimated and empirical auto-covariance matrices, i.e.

$$\mathcal{L}(\mathbf{J}, \Sigma) = \sum_{k=1}^K \lambda^k l(\mathbf{Q}^k(\mathbf{J}, \Sigma), \hat{\mathbf{Q}}^k), \quad (2)$$

where $l(\cdot)$ is the loss function between two covariance matrix, K is the number of shift we want to use for the estimation and λ is a scalar to weight among the losses for these \mathbf{Q}^k 's. Using

the gradient descent, we can estimated the description of the linear stochastic equation

$$d\mathbf{x} = (\hat{\mathbf{J}}\mathbf{x})dt + \hat{\Sigma} \cdot d\mathbf{B}_t \quad (3)$$

where $d\mathbf{B}_t$ is the standard wiener process. Analogous to the classical control representation $\dot{x}(t) = \mathbf{A}\mathbf{x}(t) + \mathbf{B}\mathbf{u}(t)$, the state transforming matrix \mathbf{A} can be modeled with the Jacobian $\hat{\mathbf{J}}$ and the control input matrix \mathbf{B} is reformulated as $\hat{\Sigma} \cdot \mathbf{B}_{\mathcal{X}}$, which simultaneously selects the control sets with $N \times K$ matrix $B_{\mathcal{X}}$ and preserves the co-varying pattern estimated from the stochastic modeling with $\hat{\Sigma}$. Consequently, we built up the linear time-invariant dynamic model for brain's functional signals as

$$\frac{d\mathbf{x}}{dt} = \hat{\mathbf{J}}\mathbf{x} + \hat{\Sigma} \cdot \mathbf{B}_{\mathcal{X}}\mathbf{u}(t) \quad (4)$$

where $uu(t)$ is the input vector to be determined. In the following section, for ease of notations, we may use $\mathbf{A} = \hat{\mathbf{J}}$ and $\mathbf{B} = \hat{\Sigma} \cdot \mathbf{B}_{\mathcal{X}}$ when there is no ambiguity.

Identification of Minimal Control Sets

Theoretically, if transition matrix \mathbf{A} for the linear system is dense, the system is almost surely controllable from a single node. But the control energy could be extremely high, which would result in unreasonable trajectories in practice. Thus here we adapt the minimum dominant set algorithm in (Sun & Ma, 2017) and define the α -minimum control set (α -MCS) as the solution of the following optimization problem.

$$\begin{aligned} & \underset{x}{\text{minimize}} && f = \sum_{i \in V} x_i \\ & \text{subject to} && x_i + \sum_{j \in V} a_{ij}x_j \geq \alpha, i, j = 1, 2, \dots, n; i \neq j. \end{aligned} \quad (5)$$

where \mathbf{A} is the transition matrix and x_i takes 0 or 1. The intuition here is that a non-driver node is called α -controllable if it has at least α weighted connectivity strength adjacent to the driver node. When the network is binary and $\alpha = 1$, it reduces to the regular MDS problem.

Controllability Measurements

Considering the special setting of control matrix, we compute the overall controllability measurement instead of the regional ones (Gu et al., 2015).

Average Controllability The average controllability of the linear stable system refers to the inverse of its H_2 -norm, which intuitively quantifies the average distance the system can reach in the state space with unit input energy. Mathematically H_2 norm is the energy of the output of the system

$$\dot{\mathbf{x}} = \mathbf{A}\mathbf{x} + \sum_i B_i \omega_i \quad (6)$$

where $\omega_i = \delta_i(t)$ is the δ -function and B_i is the i -th column control matrix in Eqn[4]. The average controllability is then

defined as

$$a_c = H_2^{-1} = \left(\sqrt{\text{trace} \left[\mathbf{B}^T \left(\int_0^{+\infty} \exp(\mathbf{A}t + \mathbf{A}^T t) dt \right) \mathbf{B} \right]} \right)^{-1} \quad (7)$$

where \mathbf{B} is the control matrix. If the average controllability is high, it means that the brain is more efficient in moving into many easily reachable states.

Global Controllability The global controllability of the linear stable system is defined as the inverse of its H_∞ -norm, which intuitively quantifies the maximal possible vector amplification with $\sin(\cdot)$ input. Mathematically, it is defined as

$$g_c = (H_\infty)^{-1} = \left(\sup_{\omega \in \mathbf{R}} \bar{\sigma}\{\mathbf{G}(j\omega)\} \right)^{-1} \quad (8)$$

where j is the virtual unit with $j^2 = -1$, $\mathbf{G}(s) = (s\mathbf{I} - \mathbf{A})^{-1}\mathbf{B}$, and $\bar{\sigma}$ denotes the largest singular value. A higher global controllability then corresponds to a easier control of the dynamics in the worst situation.

Global Synchronizability The global synchronizability refers to the inverse spread of the Laplacian eigenvalues, which intuitively measures the ability of the network's dynamics to persist in a synchronous state where all nodes have the same magnitude of activity. Mathematically, it is defined as

$$s_c = \sqrt{\frac{d^2(N-1)}{\sum_{i=1}^{N-1} |\lambda_i - \bar{\lambda}|^2}} \quad (9)$$

where λ_i is the positive eigenvalues of the Laplacian matrix \mathbf{L} with $L_{ij} = \delta_{ij} \sum_k A_{ik} - A_{ij}$ and $d = \sum_i \sum_{j \neq i} A_{ij} / N$ is the average strength of each node that plays the as a normalizer.

Results

We used the extensively preprocessed HCP data where the group-ICA decomposition was applied to obtain the parcellation and construct each region's time series. The main results here were based on the atlas of 50 regions with regard to the limited length of paper. For detailed description of the preprocessing and basic statistics of the subjects, please refer to the manual book of HCP dataset¹.

Distribution of Minimum Control Sets

We set the parameter $\alpha = 1$ and computed the 1-minimum control set for each subject. In Figure 1, we showed the z-values of the frequency of a region to appear as a control node across the population under the null hypothesis that everyone's minimum control set consist of randomly chosen regions. First we can see that the most consistent control areas are distributed broadly across the brain, including visual regions in visual cortex, temporal lobe and premotor area. Brodman area (BA) 06, 17, 18, 19, 21, 23, 40, 37, 47 are involved. These area can be divided into two categories. The

¹<https://www.humanconnectome.org>

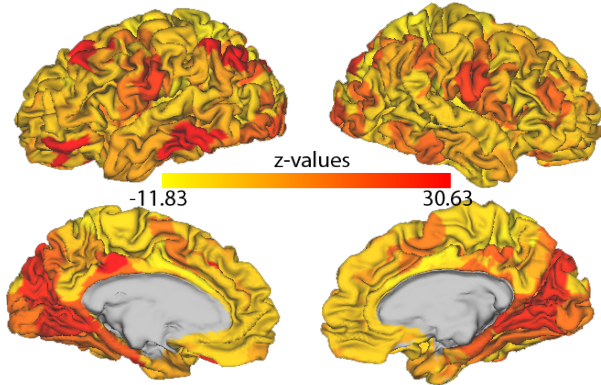


Figure 1: Nodal Distribution in Minimum Control Sets. We computed the probability of each region to be a control region under the null hypothesis where the control regions are randomly chosen, with respect to which we further calculate the z-values of the frequency of a region appearing as the control node across the full 1003 subjects. In this figure, we can see that there exist some consistent control regions in the visual cortex, temporal lobe and premotor cortex.

first group consist of sensory areas including BA 06, 17, 18, 19, which might be understood as local executive hubs. The second group are composed of integrating area including 21, 23, 40, 37, 47, which could be playing the gating roles among multiple functional modules. These functional control regions also display a certain level of similarity to the optimal controllers predicted from the structural connectivity matrices (Gu et al., 2017).

Relationship Among Controllability Measurements

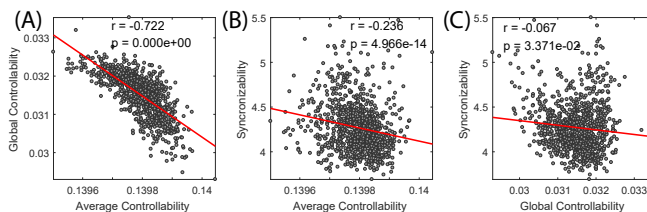


Figure 2: Correlations Among Controllability and Synchronizability for Functional Networks. In this figure, we computed the average controllability, the global controllability and the synchronizability for the fitted functional dynamics of human brains. Their relationships were quantified with the Spearman correlations. We can see that (A) the global and average controllability display very strong negative correlation which also suggests a nonlinear correspondence, while the synchronizability shows (B) a fairly significant negative correlations with the the average controllability and (C) a weakly significant negative correlations with the global controllability.

We used the square root of the full noise covariance matrix

as the control matrix \mathbf{B} and computed the average controllability, the global controllability and the synchronizability. The strong negative correlation between the average and global controllability suggests that if a brain system is efficient in reaching many states, the ability of amplifying the activation amplitude through the its dynamics is then weakened as the energy is more likely to spread over instead of accumulate in certain mode. Another observation is that the synchronizability is not as significantly correlated to either average or global controllability as show in (Tang et al., 2017). This could be caused by the different normalization on the transition matrices and distinguished setting of control matrices.

References

Betzel, R. F., Gu, S., Medaglia, J. D., Pasqualetti, F., & Bassett, D. S. (2016). Optimally controlling the human connectome: the role of network topology. *Scientific reports*, 6, 30770.

Deco, G., Tononi, G., Boly, M., & Kringelbach, M. L. (2015). Rethinking segregation and integration: contributions of whole-brain modelling. *Nature Reviews Neuroscience*, 16(7), 430.

Gilson, M., Moreno-Bote, R., Ponce-Alvarez, A., Ritter, P., & Deco, G. (2016). Estimation of directed effective connectivity from fmri functional connectivity hints at asymmetries of cortical connectome. *PLoS computational biology*, 12(3), e1004762.

Gu, S., Betzel, R. F., Mattar, M. G., Cieslak, M., Delio, P. R., Grafton, S. T., ... Bassett, D. S. (2017). Optimal trajectories of brain state transitions. *Neuroimage*, 148, 305–317.

Gu, S., Pasqualetti, F., Cieslak, M., Telesford, Q. K., Alfred, B. Y., Kahn, A. E., ... others (2015). Controllability of structural brain networks. *Nature communications*, 6, 8414.

Liu, Y.-Y., Slotine, J.-J., & Barabási, A.-L. (2011). Controllability of complex networks. *Nature*, 473(7346), 167.

Muldoon, S. F., Pasqualetti, F., Gu, S., Cieslak, M., Grafton, S. T., Vettel, J. M., & Bassett, D. S. (2016). Stimulation-based control of dynamic brain networks. *PLoS computational biology*, 12(9), e1005076.

Sun, P. G., & Ma, X. (2017). Understanding the controllability of complex networks from the microcosmic to the macrocosmic. *New Journal of Physics*, 19(1), 013022.

Tang, E., Giusti, C., Baum, G. L., Gu, S., Pollock, E., Kahn, A. E., ... others (2017). Developmental increases in white matter network controllability support a growing diversity of brain dynamics. *Nature Communications*, 8(1), 1252.

Van Essen, D. C., Smith, S. M., Barch, D. M., Behrens, T. E., Yacoub, E., Ugurbil, K., ... others (2013). The wu-minn human connectome project: an overview. *Neuroimage*, 80, 62–79.

Yan, G., Vértés, P. E., Towilson, E. K., Chew, Y. L., Walker, D. S., Schafer, W. R., & Barabási, A.-L. (2017). Network control principles predict neuron function in the caenorhabditis elegans connectome. *Nature*, 550(7677), 519.